Density-functional theory calculations of the interaction of protons and water with low-coordinated surface sites of calcium oxide

N. H. de Leeuw[1,*] and J. A. Purton[2]
[1]*Department of Chemistry, University of Reading, Whiteknights, Reading RG6 6AD, United Kingdom*
[2]*Daresbury Laboratory, Daresbury, Warrington WA4 4AD, United Kingdom*
(Received 31 August 2000; published 1 May 2001)

Electronic structure calculations, using the density-functional theory within the generalized-gradient approximation and ultrasoft pseudopotentials, have been used to investigate the interaction of protons and water with five-, four-, and three-coordinated surface sites of calcium oxide, modeled by the {100}, {310}, and microfacetted {111} surface, respectively. The calculated structural parameters of bulk CaO are found to be in good agreement with experiment. The nonhydrated {100} surface shows negligible ionic relaxation from bulk termination due to the minimal distortion of the electron density in the surface layer and electron-density plots show the crystal to be strongly ionic. On the microfacetted {111} surface redistribution of the electron density along the bond between three-coordinated calcium ion and four-coordinated oxygen ions leads to the contraction of the bond lengths and relaxation of the surface calcium into the surface. Absorption of water at the six-coordinated ions in the bulk crystal is calculated to be highly endothermic. On the five-coordinated {100} surface sites, water molecules, which were initially dissociatively adsorbed, recombine to form associatively adsorbed species with an adsorption energy of approximately 65 kJmol^{-1}, indicating physisorption. The water molecules are adsorbed by their oxygen ion to surface calcium ions but electron-density plots show additional interactions between surface anions and hydrogen atoms. On four- and three-coordinated calcium sites, adsorbed water molecules dissociate to form hydroxyl groups indicating the higher reactivity of the lower-coordinated species. The adsorption energy at the four-coordinated calcium site is higher (156 kJmol^{-1}) than at the three-coordinated site (127 kJmol^{-1}), due to bonding of the OH group to two surface calcium ions. When calcium ions are replaced by two protons each we find that the replacement energy decreases by approximately 70 kJmol^{-1} per loss of bond, from +21 kJmol^{-1} for the six-coordinated calcium ions in the bulk to −187 kJmol^{-1} for the three-coordinated calcium ions on the faceted {111} surface.

DOI: 10.1103/PhysRevB.63.195417 PACS number(s): 68.35.Bs, 61.72.Ji, 68.03.Cd

I. INTRODUCTION

Calcium oxide (CaO) is an important component of cements, for example, making up approximately 63% of some Portland cements.[1–4] It is highly reactive towards water[5,6] and this high rate of hydration may lead to the expansion of cement-based materials.[2,7] As such, it is important to understand its hydration behavior. Furthermore, CaO is a catalytic material, for example, in the reduction of NO and the decomposition of N_2O,[8–10] and hydration of its surfaces and those of many other oxides influences properties such as their catalytic behavior[11] and mechanical response.[12] For example, CaO is found to show considerable catalytic activity in the production of OH species from water and oxygen, where adsorption of water is one of the reaction steps, but not from hydrogen and oxygen, where water adsorption is not part of the reaction.[13] In addition, calcium-bearing minerals, such as calcite and hydroxyapatite, are the main components of bones and teeth, and the strength and mode of interaction of water with their surfaces determines the adsorption of proteins.[14] As a consequence of all these factors and its structural simplicity, CaO is a good model system to study adsorption behavior of water and the effect of hydration on the surface structure.

The {100} surface is the dominant plane in the cubic CaO morphology. However, it is generally agreed that low-coordinated surface ions, due to defects such as corners, kinks, and steps that are present on all experimental surfaces, are the most reactive sites towards, for example, hydration in order to increase their coordination.[15–20] In this paper, we consider the interactions of protons and water in the bulk and with low-coordinated surface sites of CaO. Hence, in addition to the planar {100} surface where all surface sites are five coordinated, we studied the {310} surface, containing four-coordinated step edge sites, and a micro-faceted {111} surface, containing three-coordinated corner sites, as models for steps and kinks on experimental {100} surfaces. By calculating the energies for adsorption of water at five-, four-, and three-coordinated surface atoms, we can identify the energetically favored configurations and investigate the assumption that low-coordinated sites should be more reactive. In addition, we have investigated the effect of removing surface calcium-oxygen pairs and replacing them by water molecules, in effect, replacing a calcium ion with two protons, with a view to evaluating the bond strengths of the variously coordinated calcium ions and studying the first steps of dissolution. The approach we have chosen to adopt is to use electronic structure calculations in order to gain information about the mode of water adsorption, associative or dissociative, and to obtain reliable estimates of surface and hydration energies.

II. COMPUTATIONAL METHODS

The total energy and structure of the CaO surfaces were determined using the Vienna *Ab Initio* Simulation Program

TABLE I. Total energy of bulk CaO as a function of plane-wave cutoff and density of *k*-point sampling.

	U_{total} of bulk CaO				
E_{cut} (eV)	300	400	500		600
K points	3×3×3	3×3×3	3×3×3	4×4×4	3×3×3
	−13.002 130	−13.004 080	−13.008 439	−13.039 017	−13.009 042
lattice parameter	4.810	4.812	4.813	4.810	4.815

(VASP).[21–24] The basic concepts of density-functional theory (DFT) and the principles of applying DFT to pseudopotential plane-wave calculations has been extensively reviewed elsewhere.[25–27] Furthermore, this methodology is well established and has been successfully applied to the study of adsorbed atoms and molecules on the surfaces of ionic materials.[28–31] Within the pseudopotential approach, only the valence electrons are treated explicitly and the pseudopotential represents the effective interaction of the valence electrons with the atomic cores. The valence orbitals are represented by a plane-wave basis set, in which the energy of the plane waves is less than a given cutoff (E_{cut}). The magnitude of E_{cut} required to converge the total energy of the system has important implications for the size of the calculation when studying elements such as oxygen, which has tightly bound $2p$ electrons. The VASP program employs ultrasoft ''Vanderbilt'' pseudo-potentials,[32,33] which allows a smaller basis set for a given accuracy. In our calculations, the core consisted of orbitals up to and including the $1s$ orbital for oxygen and the $3s$ orbital for Ca (H of course has no core). The calculations were performed within the generalized-gradient approximation, using the exchange-correlation potential developed by Perdew *et al.*,[34] whose approach has been shown to give reliable results for the energetics of adsorbates, e.g., water on TiO_2 and SnO_2 (Ref. 35), and CaF_2.[36]

For surface calculations, where two energies are compared, it is important that the total energies are well converged. The degree of convergence depends on a number of factors, two of which are the plane-wave cutoff and the density of *k*-point sampling within the Brillouin zone. We have investigated these by undertaking a number of calculations for bulk CaO with different values for these parameters (Table I). We have, by means of these test calculations, determined values for E_{cut}(500 eV) and the size of the Monkhorst-Pack[37] *k*-point mesh so that the total energy is converged to within 0.04 eV and the lattice parameter to within 0.3% of the experimental lattice parameter. In addition, we checked the convergence of the total energy for the slab calculations and found that the most suitable value of E_{cut} is the same as for the bulk materials. Also, a *k*-point mesh of 3×3×1 gave the total-energy convergence required.

The optimization of the atomic coordinates (and unit cell size/shape for the bulk material) was performed via a conjugate gradients technique which utilizes the total energy and the Hellmann-Feynman forces on the atoms (and stresses on the unit cell). We used the usual approach for modeling the surfaces using three-dimensional periodic boundary conditions by considering slabs of CaO. In addition to the *k*-point density and E_{cut} discussed above, the convergence in surface calculations is also dependent on the thickness of the slab of material and the width of the vacuum layer between the slabs. Again we checked convergence by running a series of test calculations with different slab thicknesses and gap widths. For example, Table II, shows the surface energy of the CaO {100} surface as a function of these parameters. Following these test calculations, the CaO bulk and {100} supercells used in the calculations contained four layers of CaO with 8 CaO units per simulation cell. For the {310} and {111} surfaces, the supercells contained 10 CaO units. In each case, the simulation cells were constructed so that there was a vacuum layer of approximately 20 Å between the images of the unhydrated surfaces and at least 10 Å between the images of the hydrated surfaces. Furthermore, calculations on the reactants and products were on equivalent supercells to achieve cancellation of basis set errors (this included calculations on the isolated water molecule).[28]

The surface energy (γ_s) is a measure of the thermodynamic stability of the surface with a low, positive value indicating a stable surface. The surface energy is given by

$$\gamma_s = \frac{U_s - U_b}{A}, \tag{1}$$

where U_s is the energy of the surface slab of the crystal, U_b is the energy of an equal number of atoms of the bulk crystal, and A is the surface area. The surface energies of the hydrated surfaces are evaluated with respect to liquid water, in order to determine relative surface stabilities in aqueous environment, and are calculated as follows:

$$\gamma_h = \frac{U_h - (U_b + n\mathrm{H_2O}_{(1)})}{A}, \tag{2}$$

where U_h is the energy of the hydrated surface, n is the number of adsorbed water molecules and U_b is the bulk energy as before. The energy of the liquid water molecule is taken as the sum of the calculated self energy (−1364.2

TABLE II. Surface energy of the CaO {100} surface in (Jm^{-2}) as a function of slab thickness and width of vacuum layer between the slabs.

Number of layers of crystal	Width of vacuum layer (Å)			
10	15	20	25	
3			0.622	
4	0.611	0.610	0.610	0.610
5			0.608	

$kJmol^{-1}$) of the water molecule and the experimental condensation energy (-44.0 $kJmol^{-1}$).[38]

The adsorption energies are evaluated with respect to gaseous water to enable direct comparison with experimental techniques such as temperature programmed desorption (TPD) and they are obtained from the following equation:

$$U_{\text{ads}} = \frac{U_h - (U_s + n\text{H}_2\text{O}_{(g)})}{n}, \tag{3}$$

where U_s is the energy of the surface slab as before.

In order to investigate the initial steps of dissolution of differently coordinated calcium ions from the various surfaces, we calculate the replacement of the calcium ions by two protons each. In the simulations, this process is equal to replacing a whole CaO unit by a water molecule, where the oxygen ion of the water molecule is adsorbed at the surface oxygen vacancy. The energy of the process is then given by

$$U_{\text{rep}} = \frac{(U_{\text{def}} + n\text{CaO}) - (U_s + n\text{H}_2\text{O}_{(1)})}{n}, \tag{4}$$

where U_{def} is the energy of the defective surface, containing two protons at a calcium vacancy. The energy of the replaced CaO unit is taken as the bulk lattice energy as values for hydrated calcium ions are not available due to the prohibitive computational expense involved in quantum-mechanical molecular-dynamics simulations of calcium ions in a liquid water environment. We again include liquid water in the calculations, as the dissolution of calcium ions from the crystal would take place in solution, rather than in the presence of gaseous water.

III. RESULTS AND DISCUSSION

CaO has the rock-salt structure with space-group $Fm3m$ and $a = 4.7990$ Å,[39] which we calculated to be 4.8130 Å, in adequate agreement with experiment. In the bulk, each cation and oxygen ion is six coordinate and the perfect crystal shows cubic morphology with one dominant surface, namely the {100}, containing both calcium and oxygen ions where all ions are five coordinate. In addition to the planar {100} surface, we studied the {310} surface, containing four-coordinated step edge sites and {100} terraces, and a microfaceted {111} surface, containing three-coordinated corner sites, four-coordinated edges and {100} planes. The planar {111} surface is dipolar, but on reconstruction of the surface into a microfaceted surface, as described in Watson *et al.*,[40] the dipole is removed and the reconstructed surface contains three-sided pyramids with three-coordinated ions at the apices and four-coordinated ions on the pyramid edges, while the sides of the pyramids are {100} planes. This microfaceted {111} surface has been shown experimentally to be stable through repeated etching and annealing cycles.[41] In this paper, where we were interested in modeling low-coordinated surface sites, the microfaceted {111} surface thus represents corner sites on the {100} surface.

TABLE III. Surface energies of nonhydrated CaO surfaces.

Surface	γ_s (Jm^{-2})
{100}	0.61
{310}	0.90
{111}Ca	1.49

A. Nonhydrated surfaces

Table III lists the surface energies of the nonhydrated surfaces. It is clear from the low-surface energy that the {100} surface is the most stable of the surfaces studied. The {310} surface may be thought of as a {100} surface containing monatomic steps. From Table III, we note that the effect of the presence of steps on the {100} plane, modeled by the {310} surface, is to increase the surface energy from 0.61 Jm^{-2} for the planar {100} surface to 0.90 Jm^{-2} for the {310} surface. The surface energy of the microfaceted {111} surface at 1.49 Jm^{-2} is even larger than the {310} surface. Clearly, the presence of defects on a surface, such as steps and corners, has a destabilizing effect.

The unhydrated {100} surface was described in depth in a previous paper[36] but, for the sake of completion, we will briefly review the main features. Figure 1 shows the relaxed {100} surface with a contour plot of the electron density through the CaO planes, from which it is clear that the crystal shows a strongly ionic character. It can be seen that the distortion of the electron density around the surface ions is minimal, which leads to a negligible ionic relaxation of the surface region. The interatomic distances shown in Fig. 1 indicate that relaxation leads to only a small rumpling of the surface layer, due to a larger net increase in the Ca-Ca spacing (from a bulk spacing of 4.813 to 4.848 Å) than in the O-O spacing (from 4.813 to 4.869 Å), between the topmost ions and those one unit cell below. Hence, in the relaxed surface, there is a difference in height between the surface calcium and oxygen ions of 0.02 Å with the calcium ions protruding above the oxygen ions.

Relaxation of the {310} surface, containing {100} steps, is also small with some lengthening of the calcium-oxygen bond lengths between the four-coordinated edge ions and the five-coordinated ions on the {100} plane. Figure 2 shows the relaxed microfaceted {111} surface, indicating the three-coordinated calcium ions at the pyramid apices and four-coordinated oxygen ions on the edges. Electron-density contour plots are shown through two edges of the pyramids including the three-coordinated calcium ions at the apices. There is no discernible distortion of the electron densities on the four-coordinated edges, which are still centered on the individual ions but some of the electron density around the three-coordinated corner site has been redistributed over the bonds between the calcium ion at the apex and the neighboring four-coordinated oxygen ions below, resulting in a contraction of those bond lengths from the bulk value of 2.40 to 2.16 Å. The bond lengths between these oxygen ions to the next layer of calcium ions also contract, but to a lesser extent (2.29 Å).

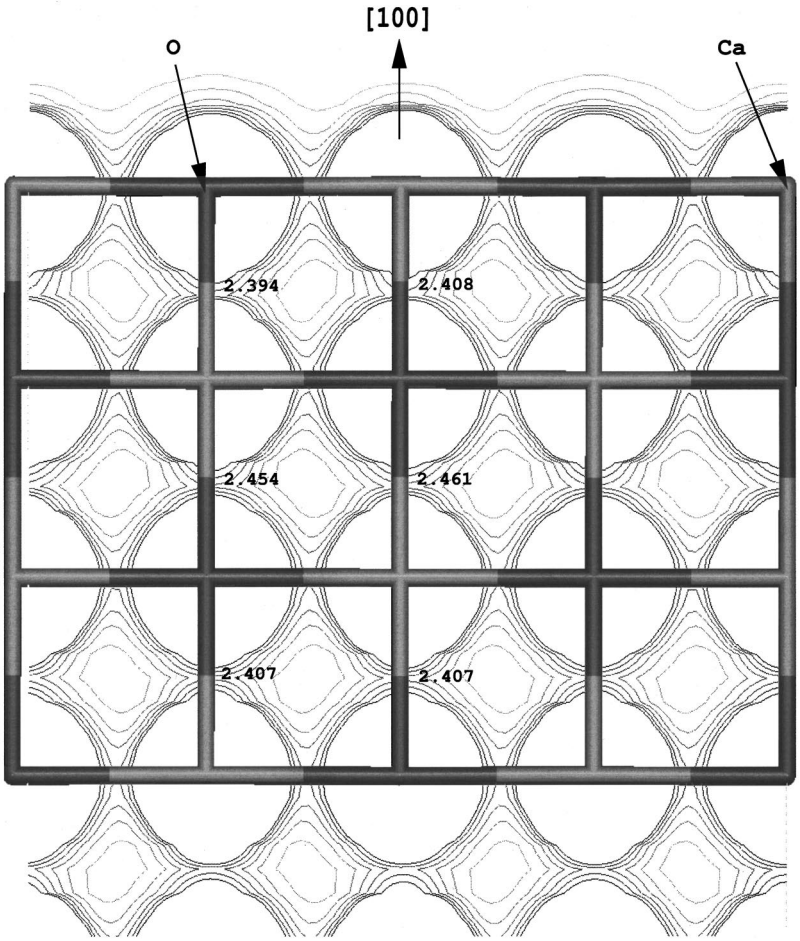

FIG. 1. Sideview of the relaxed {100} surface showing electron density contour plots and interatomic distances. (Ca=mid gray, O=dark gray, contour levels are from 0.05 to 0.35 e/Å^3 at 0.05 e/Å^3 intervals, bond lengths in Å.)

B. Hydrated surfaces

We next investigated the difference in reactivity of the variously coordinated surface sites by adsorbing gaseous water molecules in the bulk and at the three-, four-, and five-coordinated calcium ions on the CaO surfaces, and evaluated the energies of adsorption and the relaxed hydrated surface structures. As there are local minima in these hydrogen-bonded surface complexes, we used a range of different starting configurations of associatively adsorbed water molecules on the surfaces to ensure, as far as possible, that the final converged configuration would be a global rather than a local minimum-energy configuration. On the {100} surface, we considered a partial water coverage of 50% with one water molecule per two surface calcium sites. On the {310} surface, we adsorbed water molecules at the four-coordinated surface sites on the step edge, leading to a fully hydrated step edge, and on the microfaceted {111} surface, water molecules were adsorbed at each three-coordinated calcium ion. The surface and adsorption energies of the various surfaces are collected in Table IV.

Incorporation of water molecules in the bulk crystal is a highly endothermic process, costing 264 kJmol^{-1} and leading to the distortion of the crystal. However, adsorption of water at the five-coordinated {100} surface sites is exothermic and releases 65 kJmol^{-1}. Figure 3 shows a sideview of the hydrated {100} surface showing bond lengths and contour plot of the electron density through the plane of the adsorbed water molecules. The water molecules are adsorbed by their oxygen ions to surface calcium ions and the electron-density plots show this bond to have strongly ionic character. In addition, there is evidence of covalent hydrogen bonding between surface oxygen ions and one of the water molecules' protons. The surface calcium ion bonded to the water molecule's oxygen ion is pulled out of the surface by 0.04 Å with respect to the nonhydrated surface, while the oxygen ion that is not hydrogen bonded to the water molecule has moved into the surface by almost 0.1 Å.

None of the calculations of different starting configurations for the hydrated {100} surface showed the water molecules to dissociate, so in order to be certain that no lower-energy configuration with dissociatively adsorbed water molecules existed, we also simulated a hydroxylated surface as a starting configuration. A hydroxyl group was placed above a surface calcium ion with a proton bonded to a neighboring surface oxygen ion. However, the calculations showed the proton to desorb from the lattice oxygen ion and bond to the adsorbed hydroxyl group to form an associatively adsorbed water molecule. The final configuration was identical to the lowest-energy configuration of associatively adsorbed water with the same hydration energy (−65 kJmol^{-1}), giving us confidence that the lowest-energy configuration had been found. The easy reformation of dissociated water molecules indicates that there is no energy barrier to this process. Our calculations indicate that the binding of

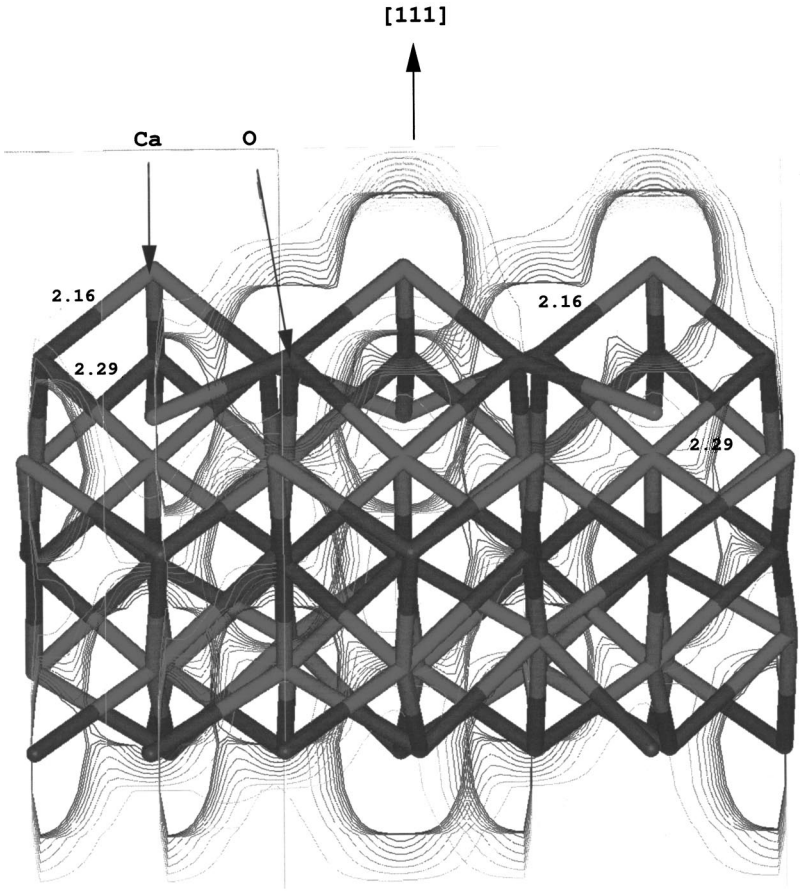

FIG. 2. Sideview of the relaxed microfaceted {111} surface showing electron density contour plots through two edges, including apex calcium ions. The three-coordinated calcium ions and four-coordinated oxygen ions are indicated in the figure by Ca and O (Ca=mid gray, O=dark gray, contour levels are from 0.05 to 0.50 e/Å^3 at 0.05 e/Å^3 intervals).

the water molecule's oxygen atom to a surface calcium atom is the main interaction. This suggests that increasing the coordination of the surface calcium ion to the bulk value, from five- to six-coordinate, is the driving force behind the adsorption. We next investigate whether water adsorption at four- and three-coordinated calcium sites rather than the five-coordinated sites of the perfect {100} surface, leads to dissociative adsorption of water, which is experimentally found to occur on CaO (e.g., Fubini *et al.*[42]).

Figure 4(a) shows an initial configuration of associatively adsorbed water molecules near the four-coordinated edge ions on the {310} surface. After electronic and ionic relaxation [Fig. 4(b)] the water molecules have dissociated and the hydroxyl group has become bonded to both a four-coordinated calcium ion on the edge and a five-coordinated calcium ion on the {100} terrace below, which now protrudes from the terrace by 0.25 Å. The proton has become bonded to a four-coordinated oxygen ion. The exothermic adsorption energy at 156 kJmol^{-1} is large, indicating a strong interaction between the water molecule and the surface. When water molecules are adsorbed at the three-coordinated calcium ions of the microfaceted {111} surface, they also dissociate. The hydroxyl group becomes only bonded to the three-coordinated calcium ion while the proton bonds to a neighboring four-coordinated oxygen ion on one of the pyramid edges. The adsorption energy at 127 kJmol^{-1} is less than for the four-coordinated calcium ions on the {310} surface above, which shows that bonding of the hydroxyl group to both a four- and a five-coordinated calcium ion outweighs bonding to one three-coordinated calcium ion.

TABLE IV. Surface and adsorption energies for the hydrated CaO surfaces.

Surface	Coordination no.	γ_h (Jm^{-2})	U_{ads}/H_2O (kJ mol^{-1})
Bulk	6		+264
{100}	5	0.45	−65
{310}	4	0.39	−156
{111}Ca	3	1.15	−127

The surface energies of all surfaces have decreased, indicating that hydration of each surface has a stabilizing effect. The {310} surface shows a particularly large decrease in surface energy of 57%, and this surface has now become the most stable of the three surfaces studied. On this surface, the adsorbed oxygen of the dissociated water molecule is approximately located at a lattice oxygen position if the step were extended. The dissociated proton and the proton of the hydroxyl group point towards the vacant calcium site next to the water molecule's oxygen ion, a surface analogue of the well-known hydrogarnet defect, where four protons are adsorbed at a silicon vacancy pointing towards the vacant site. The {100} surface that was the more stable surface when not hydrated, is much less smooth when partially covered (50%) with water molecules, hence its lower stability than the {310} surface with hydrated edge.

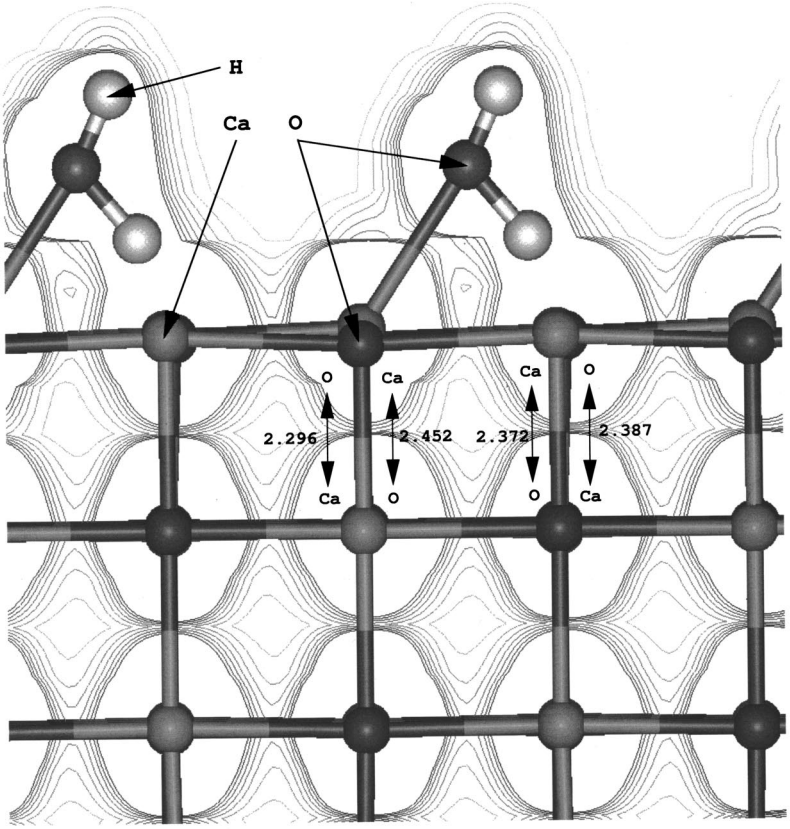

FIG. 3. Side view of the minimum energy structure of the CaO {100} surface with 50% coverage of upright adsorbed water, showing interatomic distances and contour plot of the electron density of the plane containing the water molecule, showing hydrogen bonding to surface oxygen ions. (Contour levels are from 0.05 to 0.35 e/Å^3 at 0.05 e/Å^3 intervals, Ca=pale gray, O=dark gray, H=white.)

The preference for associatively rather than dissociatively adsorbed water on the CaO {100} surface agrees qualitatively with both tight-binding calculations of hydroxylated CaO (001) slabs[43,44] and atomistic simulations of dissociative adsorption of water[45,46] where the hydration energy of a fully hydroxylated {100} surface was calculated to be large and positive (+92 kJmol^{-1}) indicating that this configuration was energetically unfavorable. In addition, previous atomistic and electronic structure calculations of water adsorption at the vacuum interface of MgO, which is isostructural with CaO, showed that dissociative adsorption is energetically unfavorable on the perfect {100} surface (e.g., Refs. 28, 45, 47, 48) and only occurs at defects and low-coordinated surface sites[12,44,49] or at the liquid water interface where H_3O^+ species are taken into account.[48] The mode of water adsorption on the {310} surface, where the hydroxyl group is bonded to both a four- and five-coordinated calcium ion agrees with hydroxylation of MgO (110) surfaces. For example, Goniakowski and Noguera using self-consistent electronic structure calculations modeled hydroxylation of a rigid MgO (110) slab, which contains four-coordinated surface sites, and found that the hydroxyl group of a water molecule binds to two magnesium ions,[44] while Langel and Parrinello showed dissociation of a water molecule at a faceted MgO (011) cluster.[12]

The calculated hydration energy of 65 kJmol^{-1} on the {100} surface suggests that physisorption is the mode of adsorption of the water molecules. Experimental work by Fubini *et al.*[42] using temperature programmed desorption (TPD) on a variety of oxide surfaces including CaO, suggest that the associative adsorption of a water molecule by its oxygen atom to a surface metal ion releases energies of between 70 and 120 kJmol^{-1}, depending on the coordination of the cation. Our calculated value for CaO falls at the bottom end of this range, which is probably due to the almost bulk-like coordination of the surface calcium ion and to its low oxidation number compared to the other metals in their study (Al, Si, Ti).

The energies of dissociative adsorption of water onto the four- and three-coordinated surface sites (−156 and −127 kJmol^{-1}, respectively) also agree well with experimentally obtained hydration energies. Again, using TPD measurements, Fubini *et al.*[42] show that water is adsorbed dissociatively on CaO with adsorption energies of 140–150 kJmol^{-1}.

C. Replacement of Ca^{2+} by protons

We next calculated the process of removing CaO units from the surfaces and replacing them by liquid water molecules. As the resulting configuration is the replacement of a calcium ion by two protons, these calculations further evaluate the reactivity of the variously coordinated sites, without the complications described above, namely that the adsorption energies depend to a large extent on the final configuration of the adsorbed water molecule and especially its oxygen atom's possible interactions with multiple surface sites, e.g., at the {310} step edge. Replacing a calcium with two protons may therefore give us a better quantitative insight into the strength of bonding of the calcium ions in the different surface environments. Table V lists the energies of replacing CaO units by liquid water molecules and we can see from those that replacing six-coordinated calcium and

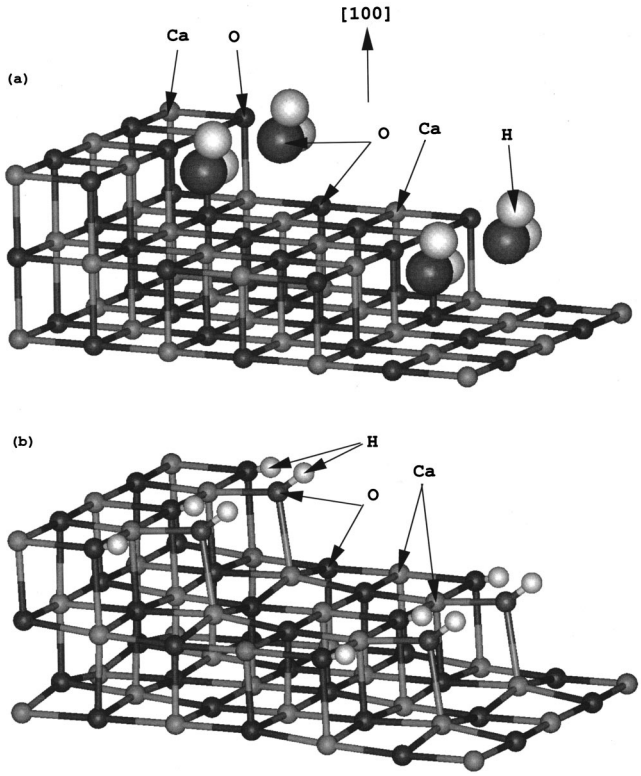

FIG. 4. Adsorption of water at the {310} surface, showing (a) unrelaxed initial configuration of undissociated water molecules and (b) relaxed configuration with dissociatively adsorbed water molecules, where the proton has become bonded to an edge oxygen ion and the hydroxyl group is coordinated by its oxygen to both an edge and a terrace calcium ion (Ca=pale gray, O=dark gray, H=white).

oxygen ions in the bulk is energetically unfavorable. We would of course expect the process of creating a defect in the perfect lattice to be endothermic and this is borne out by the calculations. Figure 5 shows the relaxed structure of the bulk crystal with protons adsorbed at the calcium vacancy, showing that the protons are pointed towards the calcium vacancy pulling the oxygen ions with them towards the vacancy.

On the {100} surface, replacement of the five-coordinated surface ions is exothermic, releasing 43 kJmol^{-1}. The surface energy (Table V) has decreased to 0.29 Jm^{-2} and the {100} surface has once more become the most stable of the three defective surfaces. The {310} surface, where a CaO group on the edge is replaced by a water molecule, is identical to the hydrated {310} edge [Fig. 4(b)] and the relaxed surface configurations and calculated surface energies (0.38 Jm^{-2}) are the same for the two simulations. Even though the two {310} surfaces are indistinguishable when 'real' surfaces are considered, the simulation cells for the two calculations are not the same and the identical results for the two cells further shows that the sizes of the simulation cells are adequate. As expected from its higher reactivity towards water adsorption discussed in the section above, the four-coordinated ions at the step edge ($U_{rep}=-111$ kJmol^{-1}) are more amenable to replacement than the five-coordinated ions on the planar {100} surface.

TABLE V. Surface and replacement energies of replacement of CaO units by water molecules.

Surface	Coordination no.	γ_r (Jm^{-2})	U_{rep}/H_2O (kJ mol^{-1})
Bulk	6		+21
{100}	5	0.29	−43
{310}	4	0.38	−111
{111}Ca	3	0.73	−187

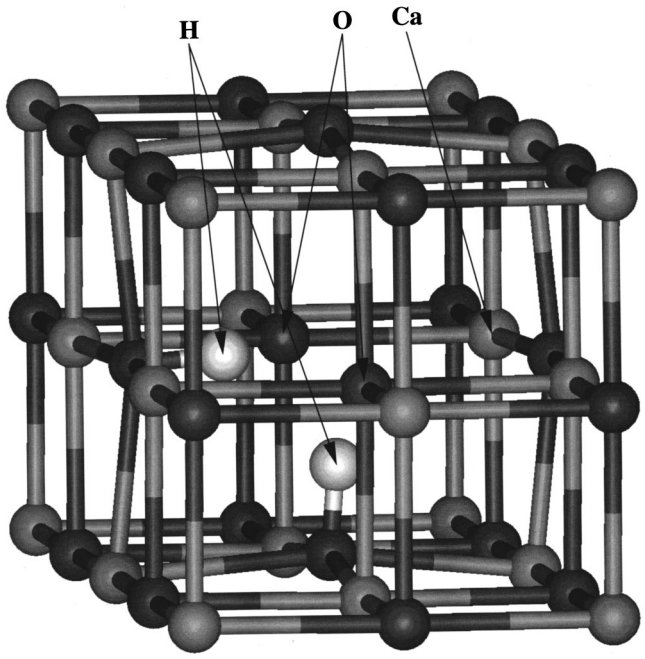

FIG. 5. Minimum energy structure of bulk CaO crystal with one six-coordinated calcium ion replaced by two protons, showing relaxation of the resulting hydroxyl groups towards the cation vacancy.

The surface energy of the microfaceted {111} surface has been halved by the replacement of the three-coordinated calcium ions with two protons each. The surface resulting from ''dissolving'' the apex calcium ions is much smoother than the original surface that leads to its enhanced stability. Contrary to the adsorption of water at the {111} and {310} surfaces described above, this time the reaction energy at the three-coordinated ions (−187 kJmol^{-1}) is more exothermic than at the four-coordinated edge ions (−111 kJmol^{-1}).

IV. CONCLUSION

We have used density-functional theory simulations using the pseudopotential approach to investigate the hydration of the bulk crystal and the {100}, {310}, and microfaceted {111} surfaces of CaO. The experimental crystal structure parameters of CaO are reproduced adequately by the calculations. An electron-density plot of the {100} surface shows the material to have a strongly ionic character without discernible distortion in the surface layer with respect to bulk layers, leading to minimal ionic relaxation of the {100} surface. Re-

laxation of the microfaceted {111} surface is more pronounced, due to the redistribution of the electron density along the bonds between the three-coordinated apex calcium ions and their neighboring four-coordinated oxygen ions. The three-coordinated calcium ions at the pyramid apices move into the surface through contraction of the Ca-O bonds in the topmost two layers.

On adsorbing water in the bulk and onto the {100} surface, we find that associative adsorption of water is energetically preferred. Absorption of a water molecule in the bulk lattice is calculated to be an endothermic process, while the adsorption energy at the {100} surface indicates physisorption. The water molecules adsorb by their oxygen ions to the surface calcium ions, but an electron-density contour plot through the plane of the water molecule adsorbed on the {100} surface shows a hydrogen-bonding interaction between a surface oxygen ions and one of the water molecule's hydrogen atoms. The energetic preference for associatively adsorbed water is confirmed by performing simulations on dissociatively adsorbed water molecules on the {100} surface, which reassemble during the minimization process indicating that this surface is not amenable to hydroxylation. In addition, there appears to be no energy barrier for reformation of the water molecules.

At the four- and three-coordinated ions of the {310} and microfaceted {111} surfaces, dissociative adsorption occurs. However, the adsorption energies, which are in good agreement with experimentally found hydration energies, are not dependent on the coordination of the surface ions but rather on the final configuration and coordination of the adsorbed water molecule. At the four-coordinated edge ions the hydroxyl group bonds to two calcium ions, one at the edge and one on the {100} terrace below the edge. This dual coordination, which agrees with calculations of hydroxylated MgO (110) surfaces, leads to a more favorable adsorption energy than at the three-coordinated corner ions where the hydroxyl group is only bonded to one calcium ion. The protons on both these surfaces become bonded to four-coordinated oxygen ions.

When calcium ions are replaced by protons in the bulk and at the surfaces, we find a clear relation between cation coordination and replacement energy. The energy released by replacing a calcium ion by two protons increases by 65–75 $kJmol^{-1}$ for the loss of each successive bond, from six coordinated in the bulk to three-coordinated calcium ions at the microfaceted {111} surface. In future work, we would like to extend these replacement calculations to MgO and quartz to investigate whether the energies have a qualitative relation to bond strengths in different materials.

*Email address: n.h.deleeuw@reading.ac.uk

[1] P. S. De Silva and F. P. Glasser, Cem. Concr. Res. **23**, 627 (1993).
[2] V. Kasselouri, P. Tsakiridis, Ch. Malami, B. Georgali, and C. Alexandridou, Cem. Concr. Res. **25**, 1726 (1995).
[3] E. Henderson and J. E. Bailey, J. Mater. Sci. **28**, 3681 (1993).
[4] P. Lu and J. F. Young, J. Am. Ceram. Soc. **76**, 1329 (1993).
[5] M. Bailes, B. Fubini, and F. S. Stone, Stud. Surf. Sci. Catal. **48**, 31 (1989).
[6] H. S. Song and C. H. Kim, Cem. Concr. Res. **20**, 815 (1990).
[7] S. Chatterji, Cem. Concr. Res. **25**, 51 (1995).
[8] F. Acke and I. Panas, J. Phys. Chem. B **102**, 5127 (1998).
[9] A. Snis and H. Miettinen, J. Phys. Chem. B **102**, 2555 (1998).
[10] K. D. Fliatoura, X. E. Verykios, C. N. Costa, and A. M. Efstathiou, J. Catal. **183**, 323 (1999).
[11] H. Dunski, W. K. Jozwiak, and H. Sugier, J. Catal. **146**, 166 (1994).
[12] W. Langel and M. Parrinello, Phys. Rev. Lett. **73**, 504 (1994).
[13] S. Noda, M. Nishioka, A. Harano, and M. Sadakata, J. Phys. Chem. B **102**, 3185 (1998).
[14] S. P. Nair, S. Meghji, M. Wilson, I. Nugent, A. Ross, A. Ismael, N. K. Bhudia, M. Harris, and B. Henderson, Br. J. Rheumatol. **36**, 328 (1997).
[15] C. F. Jones, R. A. Reeve, R. Rigg, R. L. Segall, R. St. C. Smart, and P. S. Turner, J. Chem. Soc., Faraday Trans. 1 **80**, 2609 (1984).
[16] F. S. Stone, J. Solid State Chem. **12**, 271 (1975).
[17] E. A. Colbourn and W. C. Mackrodt, Surf. Sci. **117**, 571 (1982).
[18] H. Kobayashi, M. Yamaguchi, and T. Ito, J. Phys. Chem. **94**, 7206 (1990).
[19] T. Ito, T. Tashiro, M. Kawasaki, T. Watanabe, K. Toi, and H. Kobayashi, J. Phys. Chem. **95**, 4476 (1991).
[20] M. A. Nygren and L. G. M. Petterson, J. Chem. Phys. **105**, 9339 (1996).
[21] G. Kresse and J. Hafner, Phys. Rev. B **47**, 558 (1993).
[22] G. Kresse and J. Hafner, Phys. Rev. B **49**, 14 251 (1994).
[23] G. Kresse and J. Furthmller, Comput. Mater. Sci. **6**, 15 (1996).
[24] G. Kresse and J. Furthmller, Phys. Rev. B **54**, 11 169 (1996).
[25] R. Jones and O. Gunnarsson, Rev. Mod. Phys. **61**, 689 (1989).
[26] M. Payne, M. Teter, D. Allan, T. Arias, and J. Joannopoulos, Rev. Mod. Phys. **64**, 1045 (1992).
[27] M. Gillan, Contemp. Phys. **38**, 115 (1997).
[28] K. Refson, R. A. Wogelius, D. G. Fraser, M. C. Payne, M. H. Lee, and V. Milman, Phys. Rev. B **52**, 10 823 (1995).
[29] P. J. D. Lindan, J. Muscat, S. Bates, N. M. Harrison, and M. Gillan, Faraday Discuss. **106**, 135 (1997).
[30] P. J. D. Lindan, N. M. Harrison, and M. J. Gillan, Phys. Rev. Lett. **80**, 762 (1998).
[31] S. P. Bates, G. Kresse, and M. J. Gillan, Surf. Sci. **409**, 336 (1998).
[32] D. Vanderbilt, Phys. Rev. B **41**, 7892 (1990).
[33] G. Kresse and J. Hafner, J. Phys.: Condens. Matter **6**, 8245 (1994).
[34] J. P. Perdew, J. A. Chevary, S. H. Vosko, K. A. Jackson, M. R. Pederson, D. J. Singh, and C. Fiolhas, Phys. Rev. B **46**, 6671 (1992).
[35] J. Goniakowski and M. J. Gillan, Surf. Sci. **350**, 145 (1996).
[36] N. H. de Leeuw, J. A. Purton, S. C. Parker, G. W. Watson, and G. Kresse, Surf. Sci. **452**, 9 (2000).
[37] H. J. Monkhorst and J. D. Pack, Phys. Rev. B **13**, 5188 (1976).
[38] D. A. Johnson, *Some Thermodynamic Aspects of Inorganic Chemistry* (Cambridge University, Cambridge, England, 1982).
[39] W. A. Deer, R. A. Howie, and J. Zussman, *Introduction to the*

Rock Forming Minerals (Longman, Harlow, United Kingdom, 1992).
[40] G. W. Watson, E. T. Kelsey, N. H. de Leeuw, D. J. Harris, and S. C. Parker, J. Chem. Soc., Faraday Trans. **92**, 433 (1996).
[41] V. E. Henrich, Surf. Sci. **57**, 385 (1976).
[42] B. Fubini, V. Bolis, M. Bailes, and F. S. Stone, Solid State Ionics **32**, 258 (1989).
[43] C. Noguera, J. Goniakowski, and S. Bouette-Russo, Surf. Sci. **287**, 188 (1993).
[44] J. Goniakowski and C. Noguera, Surf. Sci. **330**, 337 (1995).
[45] N. H. de Leeuw, G. W. Watson, and S. C. Parker, J. Phys. Chem. **99**, 17 219 (1995).
[46] N. H. de Leeuw and S. C. Parker, Res. Chem. Intermed. **25**, 195 (1999).
[47] C. A. Scamehorn, A. C. Hess, and M. I. McCarthy, J. Chem. Phys. **99**, 2786 (1993).
[48] M. A. Johnson, E. V. Stefanovich, T. N. Truong, J. Gnster, and D. W. Goodman, J. Phys. Chem. B **103**, 3391 (1999).
[49] N. H. de Leeuw, G. W. Watson, and S. C. Parker, J. Chem. Soc., Faraday Trans. **92**, 2081 (1996).